

IUE OBSERVATIONS OF PHASE-DEPENDENT VARIATIONS IN WN+O SYSTEMS

G. KOENIGSBERGER

Pennsylvania State University

AND

L. H. AUER

Los Alamos National Laboratory

Received 1985 January 17; accepted 1985 April 5

ABSTRACT

IUE observations of six WN+O Wolf-Rayet (W-R) systems are reported. The periodic variations in five of the six systems are shown to result primarily from selective atmospheric eclipses of the O star continuum by the W-R wind. An optical depth distribution of the form $\tau \propto r^{-1}$ is suggested for $r \gtrsim 14 R_{\odot}$. The presence of the N IV ionization stage out to at least $\sim 60 R_{\odot}$ is consistent with the proposed constant ionization structure in WN winds (Willis). Phase-dependent variations in the C IV 1550 absorption components in V444 Cyg, HD 90657, and HD 211853 are interpreted as wind-wind collision effects.

Subject headings: stars: eclipsing binaries — stars: Wolf-Rayet — ultraviolet: spectra

I. INTRODUCTION

Variations of emission-line profiles in the visible spectra of Wolf-Rayet (W-R) stars have long been known to occur. Some of the variations, such as those observed in γ Vel (Bahng 1975; Jeffers, Weller, and Sanyal 1973) may result from instabilities in the W-R's mass flow. However, many of the profile variations in the W-R binaries are strongly phase dependent, and, therefore, related to the presence of the companion. For example, in HD 211853 (Hiltner 1945; Ganesh and Bappu 1968), CQ Cep (Bappu and Sinvhal 1955), HD 90657 (Niemela 1976), V444 Cyg (Wilson 1945), and HD 50896 (Firmani *et al.* 1980) the changes in the structure of the He II $\lambda 4686$ emission are periodic on time scales of the binary orbit. In addition, in some of the binary systems, certain lines have stronger absorption components at phases in which the W-R star is in front of its companion. This is particularly true in V444 Cyg (Münch 1950) where the shortward-shifted absorption components of N V $\lambda 4603$, 19 are strong when the W-R is in front and become weak or disappear completely at the opposite phase. Furthermore, N IV $\lambda 3483$ and He I $\lambda 4471$ in V444 Cyg (Münch 1950) and C III-IV $\lambda 4650$ in CV Ser (Cowley, Hiltner, and Berry 1971; Massey and Niemela 1981) develop shortward-shifted absorption components only when the W-R is in front of the O companion.

The periodic variations have frequently been attributed to the presence of gas stream flowing through the Lagrangian points of the gravitational equipotentials of the binary systems (Sahade 1958; Kuhl 1968). However, WR+O binary systems do not conform to a simple Roche lobe overflow geometry. First of all, the large wind velocities prevent the equipotential surfaces from having a significant effect on the mass outflow (Castor 1970a). Second, we now know that all O stars have considerable mass outflows of their own, leading to a wind-wind collision in the region between the W-R and O members of binary systems. The energy released in this collision (Priluskii and Usov 1976; Cooke, Fabian, and Pringle 1978) renders any interpretation in terms of "cool" streams of gas extremely unlikely.

Münch (1950) suggested that the strengthening of P Cyg absorption components in V444 Cyg at primary eclipse (W-R

in front) results from absorption of the O star's continuum radiation by atoms in the W-R wind. This interpretation in terms of selective atmospheric eclipses is consistent with recent *IUE* observations of V444 Cyg (Eaton, Cherepashchuk, and Khaliullin 1982) and γ Vel (Willis *et al.* 1979), and has been applied to optical emission-line variability in V444 Cyg and CQ Cep (Khaliullin 1973; Khaliullin and Cherespaschuk 1976; Cherepashchuk 1982).

Because the absorption components of P Cyg features are produced in the outward flowing material between the observer and a continuum source, they contain information regarding the density and velocity structures along the line of sight to the source. If the eclipse interpretation is appropriate, a progressive strengthening of the P Cyg absorptions should be visible as the O star is occulted by growing column density of W-R wind material. Thus, given the orbital parameters, an empirical determination of the optical depth structure in the W-R wind should be possible. This would be very useful for obtaining further insight into the structure of W-R winds. A knowledge of wind structure is necessary in order to establish the mechanisms responsible for the large mass-loss rates derived for W-R stars (Barlow, Smith, and Willis 1981).

In this paper, we investigate the use of periodic emission-line profile variations to derive information regarding the structure of winds in W-R stars.

We report periodic spectral variations at ultraviolet (UV) emission-line frequencies in systems containing a W-R star of the nitrogen sequence (WN) and an O star companion. We show that the major variability indeed results from selective atmospheric eclipses and a first-order empirical determination of the line optical depth distribution in the WN winds is determined. In addition, periodic changes in the C IV $\lambda 1550$ line are interpreted as evidence for wind-wind collisions in WN+O binary systems.

II. OBSERVATIONS AND MEASUREMENTS

Table 1 lists the W-R stars selected for this study, along with the available orbital parameters. The systems all contain an early WN component (WN 4-6), have short orbital periods, are bright enough for short exposure times, and most are

TABLE 1
 OBSERVED SYSTEMS

| Parameter | V444 Cyg ^{a,b,c} | HD 90657 ^d | HD 186943 ^e | HD 211853 ^e | HD 94546 ^f | HD 193077 ^g |
|------------------------------|---------------------------|-----------------------|------------------------|------------------------|-----------------------|------------------------|
| Spectrum | WN 5+O6 | WN 4+O4-6 | WN 4+O9 V | WN 6+O | WN 4+O | WN 6+O |
| Period | 4 ^d 2124 | 8.255 | 9.5548 | 6.6884 | 4.83 | 2.31 |
| $a \sin i (R_{\odot})$ | 35 | 50 | 55 | | 38 | ... |
| i | 78° | 46°-67° | 70° | (70°) | ... | ... |
| $T_0(-2,400,000)$ | 41,164.332 | 43,915.654 | 43,789.24 | 43,690.32 | 43,140. | ... |

^a Cherepashchuk and Khaliullin 1973.

^b Cherepashchuk 1975.

^c Münch 1950.

^d Niemela and Moffat 1982.

^e Massey 1981.

^f Niemela (1982, private communication).

^g Lamontagne *et al.* 1982.

known to undergo periodic profile variations in their optical spectra. Two of the systems, V444 Cyg and HD 211853, are eclipsing binaries, although the latter is apparently part of a quadruple system (Massey 1981). Thus, orbital elements for this system may be uncertain. HD 193077 is a proposed triple system, containing a WN 6 + compact object in a close orbit ($P = 2.3$), both of which are in orbit about an O star at a considerable distance (Lamontagne *et al.* 1982).

The observations were carried out with the *IUE* at NASA/GSFC with the short wavelength prime (SWP) camera (1200–1900 Å), through the large aperture and in the low-dispersion mode. Exposure times were chosen so as to optimize the count levels in the continuum and in the N IV $\lambda 1718$ emission line. Hence, He II $\lambda 1640$ was just saturating on most exposures. Low-dispersion images were decided upon in order to maximize phase coverage of the six systems, obtain good signal to noise images of the weaker targets, and permit accurate positioning of the continuum.

The six targets listed in Table 1 were observed on each of six observing shifts, and an additional 21 SWP images of V444 Cyg were drawn from the archives of the National Space Science Data Center.

Data reduction was conducted at the Regional Data Analysis Facility (RDAF) NASA/GSFC. Standard *IUE* procedures were employed to obtain absolute fluxes, equivalent widths, and wavelength positions. Additional flux and wavelength measurements were made directly from CalComp plots. Recorded exposure times of trailed images were divided by 1.07 to correct for the adjusted trail rate (Panek 1981). No correction for interstellar reddening has been applied.

Since we intend to analyze the variability, it is important to discern fluctuations due to the detection and reduction procedures from the actual spectral variations. In addition, we require an estimate of the uncertainties in the measurements of velocity, flux, and equivalent width.

As pointed out by Ayres (1982), a sequence of several images exposed to the same count levels can be used to determine the standard deviation of the individual fluxes about the mean taking automatically into account errors resulting from the original image processing. We applied this procedure to derive a quantitative estimate of the uncertainties in the measurements using the eight images of HD 193077. No variability greater than 5% was detected in this source in our low-dispersion spectra. Thus, it serves as a “standard” for comparison with the other more variable sources. The *IUE* spectra have been confirmed to be reliable on the 5% level.

For all other systems, substantial variability is evident in all emission features, with the exception of the semiforbidden transition of N IV at 1486 Å. Severe line blending impedes accurate assessment of the variations, except in the case of the line at 1718 Å, which is relatively free of blending effects. Thus, we will restrict our analysis to this line and consider its variations to be representative of those occurring in other lines.

We should note in passing the lack of variability seen in the low-dispersion spectra of HD 193077 is inconsistent with the variability seen in the other systems. It appears to imply that the WN is not, in fact, in a close, low-inclination orbit in conjunction with an O star.

In Table 2 we list the measured quantities for all of the *IUE* images, identified by their SWP numbers, listed in column (1). SWP numbers smaller than 15,500 correspond to images drawn from archives of the National Space Science Data Center. An asterisk indicates a trailed image. In column (2) we list the orbital phase computed from the ephemerides in Table 1. The measured quantities derived from the 1718 Å feature are in the remaining columns. Columns (3)–(5), (8), and (9) lists the positions (in 10^2 km s^{-1}) corresponding to the largest expansion velocity represented by the line (i.e., the intersection with the continuum) and the positions of minimum and maximum flux in the P Cygni feature. The following notation is used: V_1 and V_3 correspond to the blue and red wings, respectively, of the absorption component; V_5 to the red wing of the emission component; and V_A and V_E to the minimum in the absorption and the maximum in the emission, respectively. Columns (6) and (10) contain the monochromatic flux (in units of $10^{-13} \text{ ergs cm}^{-2} \text{ s}^{-1} \text{ \AA}^{-1}$) of the absorption (F_A) and emission (F_E) extrema, respectively. Columns (7) and (11) contain the corresponding equivalent widths.

In the 38 images obtained during our observing run, we also measured flux in the continuum region around 1825 Å, which is relatively free of lines. The averages, plus or minus standard deviations for this quantity (F_{1825}), and for V_A , V_E , F_A , F_E , W_A , and W_E are listed in Table 3. The percent sign indicates percent variations; i.e., (s.d.)/mean.

According to the results in Table 3, we can state that, in comparison to HD 193077, there is significant line flux and equivalent width variability in V444 Cyg, HD 90657, and HD 211853, and moderate variability in HD 186943 and HD 94546. On the other hand, little or no continuum variability is detected in any of these objects.

It is interesting to note the large difference between the velocity standard deviations in HD 193077 and the velocity

standard deviations derived for the rest of the sources. Specifically, we find the standard deviation of relative measurements in HD 193077 to be $\sim 80 \text{ km s}^{-1}$. This illustrates the remarkable stability of the *IUE* wavelength calibration procedures and quantifies the uncertainty in establishing the position of extrema in the P Cygni profiles. Although the velocity measurements are limited in general by the $\sim 6 \text{ \AA}$ resolution of the low-dispersion spectra, the positions of extrema (i.e., line centers) can be determined with higher precision. Furthermore, the stability of the wavelength calibration permits relative flux measurements at a given wavelength to be obtained with considerable reliability. We emphasize that our present analysis will require only relative flux and wavelength measurements. The velocity standard deviations in all the other sources are $\sim 200\text{--}500 \text{ km s}^{-1}$, comparable with typical orbital velocities reported for W-R stars.

III. ULTRAVIOLET VARIATIONS

Figures 1a–1c illustrate the UV spectra at individual orbital phases of the three most variable sources. The variations are very similar and can be described as follows:

1. The P Cygni structure of N IV $\lambda 1718$ undergoes a transition from an emission accompanied by a weak or absent absorption component when the O star is in front of the W-R ($\phi \approx 0.5$) to weak or absent emission with a very intense absorption component at the opposite phase.

2. He II $\lambda 1640$ develops a shortward-shifted absorption component at $\phi \approx 0$, but no absorption is apparent at other phases.

3. The apparent continuum region shortward of $\sim 1500 \text{ \AA}$ is significantly depressed at $\phi \approx 0$. In the more extreme cases, this constitutes a variation of 45% in flux level, while no varia-

TABLE 2
N IV $\lambda 1718$ MEASURED LINE PARAMETERS

| SWP (1) | PHASE (2) | ABSORPTION | | | | | EMISSION | | | |
|------------|--------------|----------------|--------------|--------------|----------------|----------------|--------------|--------------|---------------|---------------|
| | | V_1^a (3) | V_A (4) | V_3 (5) | F_A^b (6) | W_A^c (7) | V_E (8) | V_5 (9) | F_E (10) | W_E (11) |
| V444 Cygni | | | | | | | | | | |
| 13832 | 0.917 | -32. | -91. | +1. | 8.3 | 4.8 | +9 | 30. | 21.1 | 1.9 |
| 14714 | 0.572 | -30. | -23. | -18. | 15.0 | 0.5 | -5. | 14. | 26.6 | 6.7 |
| 15380 | 0.852 | -23. | -11. | -3. | 11.7 | 1.9 | +8. | 22. | 24.7 | 4.0 |
| 15387 | 0.992 | -22. | -10. | -1. | 4.7 | 4.1 | +4. | 15. | 17.1 | 2.3 |
| 15388 | 0.998 | -21. | -10. | -1. | 4.8 | 3.9 | +5. | 20. | 17.1 | 2.8 |
| 15389 | 0.003 | -23. | -12. | -3. | 4.5 | 3.9 | +4. | 18. | 16.9 | 3.1 |
| 15390 | 0.008 | -20. | -11. | -1. | 4.6 | 4.4 | +5. | 18. | 17.0 | 2.0 |
| 15391 | 0.015 | -23. | -10. | -1. | 5.6 | 4.2 | +7. | 20. | 18.2 | 2.2 |
| 15392 | 0.020 | -21. | -10. | 0. | 4.9 | 4.2 | +7. | 18. | 17.1 | 1.8 |
| 15394 | 0.030 | -20. | -10. | -1. | 5.7 | 3.9 | +5. | 18. | 17.5 | 2.1 |
| 15396 | 0.051 | -17. | -6. | +4. | 5.5 | 4.3 | +9. | 18. | 16.9 | 0.9 |
| 15397 | 0.056 | -25. | -8. | +2. | 6.4 | 4.1 | +9. | 16. | 17.4 | 1.2 |
| 15399 | 0.066 | -21. | -7. | +4. | 6.5 | 4.1 | +9. | 18. | 18.1 | 0.9 |
| 15400 | 0.071 | -39. | -8. | +7. | 7.0 | 6.1 | ... | ... | ... | 0.0 |
| 15401 | 0.076 | -24. | -6. | +5. | 7.2 | 4.8 | +8. | 18. | 18.4 | 0.5 |
| 15402 | 0.081 | -19. | -7. | +4. | 7.4 | 3.5 | ... | ... | ... | ... |
| 15403 | 0.085 | -24. | -7. | +4. | 7.2 | 4.7 | +12. | 20. | 18.8 | 0.9 |
| 15405 | 0.098 | -25. | -7. | +3. | 8.5 | 4.1 | +12. | 23. | 18.7 | 1.0 |
| 15406 | 0.103 | -23. | -7. | +5. | 7.7 | 3.9 | +11 | 23. | 19.3 | 2.2 |
| 15407 | 0.108 | -22. | -8. | +2. | 7.9 | 4.1 | +10 | 23. | 21.4 | 2.0 |
| 15408 | 0.114 | -21. | -7. | +4. | 8.5 | 3.9 | +11. | 22. | 20.7 | 2.0 |
| 15580 | 0.589 | ... | ... | -13. | ... | 0. | 0. | 18. | 25.0 | 5.1 |
| 15588 | 0.835 | -24. | -13. | -4. | 10.0 | 2.6 | +7. | 23. | 23.9 | 2.9 |
| 15602 | 0.073 | -20. | -6. | 0. | 7.2 | 3.2 | +11. | 24. | 18.9 | 1.8 |
| 15615* | 0.491 | ... | ... | -10. | ... | 0. | +5. | 24. | 19.4 | 3.9 |
| 15628* | 0.736 | -31. | -13. | -6. | 11.4 | 2.0 | +2. | 23. | 24.9 | 4.3 |
| 15644* | 0.974 | -22. | -11. | -4. | 6.3 | 3.3 | +5. | 16. | 15.8 | 1.2 |
| HD 90657 | | | | | | | | | | |
| 15576 | 0.70 | -24. | -15. | -6. | 6.7 | 1.4 | +2. | 18. | 11.6 | 2.8 |
| 11584 | 0.83 | -24. | -13. | -4. | 6.3 | 2.1 | +5. | 18. | 11.9 | 2.0 |
| 15598 | 0.95 | -40. | -11. | +7. | 4.8 | 4.7 | +13. | 23. | ... | 0.6 |
| 15618 | 0.19 | -29. | -9. | 0. | 6.3 | 2.7 | +9. | 30. | 14.1 | 0.6 |
| 15630* | 0.31 | -20. | -9. | -2. | 6.3 | 1.9 | +9. | 31. | 12.4 | 4.5 |
| 15646 | 0.43 | -29. | -13. | -4. | 7.8 | 1.4 | +7. | 24. | 12.2 | 2.9 |
| HD 186943 | | | | | | | | | | |
| 15578 | 0.11 | -23. | -12. | -5. | 5.7 | 1.8 | +7. | 21. | 11.7 | 4.3 |
| 15586 | 0.22 | -29. | -15. | -2. | 5.8 | 1.8 | +7. | 31. | 13.7 | 5.8 |
| 15600 | 0.32 | -24. | -15. | -4. | 7.4 | 0.9 | +5. | 20. | 14.0 | 4.4 |
| 15616 | 0.52 | ... | ... | -13. | ... | ... | +8. | 23. | 13.4 | 5.6 |
| 15627 | 0.62 | -26. | -17. | -9. | 7.3 | 1.1 | 0. | 18. | 13.3 | 5.5 |
| 15643 | 0.72 | -35. | -20. | -10. | 7.0 | 1.2 | +2. | 23. | 13.7 | 5.1 |

TABLE 2—Continued

| SWP (1) | PHASE (2) | ABSORPTION | | | | | EMISSION | | | |
|--------------|---------------------|----------------|--------------|--------------|----------------|----------------|--------------|--------------|---------------|---------------|
| | | V_1^a (3) | V_A (4) | V_3 (5) | F_A^b (6) | W_A^c (7) | V_E (8) | V_5 (9) | F_E (10) | W_E (11) |
| HD 211853 | | | | | | | | | | |
| 15579 | 0.38 | -20. | -9. | 0. | 12.2 | 1.4 | +9. | 41. | 21.2 | 5.2 |
| 15587 | 0.53 | -18. | -9. | -4. | 13.9 | 0.4 | +11. | 35. | 18.9 | 4.0 |
| 15601 | 0.68 | -26. | -15. | -2. | 14.5 | 0.8 | +7. | 23. | 20.6 | 3.0 |
| 15617* | 0.96 | -33. | -11. | +5. | 9.0 | 2.9 | +20. | 45. | 16.3 | 1.6 |
| 15629* | 0.11 | -26. | -9. | +2. | 10.4 | 2.2 | +16. | 35. | 16.5 | 2.2 |
| 15645 | 0.26 | -26. | -11. | -2. | 11.2 | 2.0 | +7. | 27. | 20.4 | 3.5 |
| HD 94546 | | | | | | | | | | |
| 15577 | (0.02) ^d | ... | ... | -10. | ... | 0. | +3. | 24. | 9.0 | (7.0) |
| 15585 | (0.23) | -20. | -14. | -8. | 4.4 | 1.1 | +2. | 21 | 8.9 | 5.9 |
| 15599 | (0.43) | -22. | -11. | -4. | 4.0 | 1.4 | +7. | 34. | 7.9 | 5.6 |
| 15619 | (0.85) | -16. | -10. | -5. | 4.4 | 0.7 | +6. | 23. | 9.3 | 6.5 |
| 15631 | (0.06) | -23. | -17. | -9. | 5.2 | 0.4 | +4. | 19. | 9.5 | 6.2 |
| 15647 | (0.27) | -23. | -13. | -6. | 4.3 | 1.4 | +4. | 17. | 9.3 | 5.6 |
| HD 193077 | | | | | | | | | | |
| 15575* | ... | -21. | -10. | -5. | 29. | 1.1 | +4. | 21. | 62.6 | 6.1 |
| 15583 | ... | -20. | -10. | -4. | 30. | 1.2 | +4. | 22. | 64.5 | 5.2 |
| 15589 | ... | -20. | -11. | -4. | 27. | 1.5 | +5. | 17. | 62.0 | 6.0 |
| 15597 | ... | -18. | -12. | -4. | 28. | 1.2 | +4. | 22. | 63.0 | 5.7 |
| 15603 | ... | -20. | -10. | -5. | 28. | 1.3 | +6. | 21. | 53.0 | 5.4 |
| 15614* | ... | -19. | -11. | -4. | 28. | 1.5 | +4. | 21. | 66.4 | 5.5 |
| 15626 | ... | -21. | -10. | -3. | 32. | 1.2 | +3. | 19. | 67.5 | 5.8 |
| 15642* | ... | -22. | -10. | -5. | 29. | 1.3 | +5. | 23. | 65.4 | 6.0 |

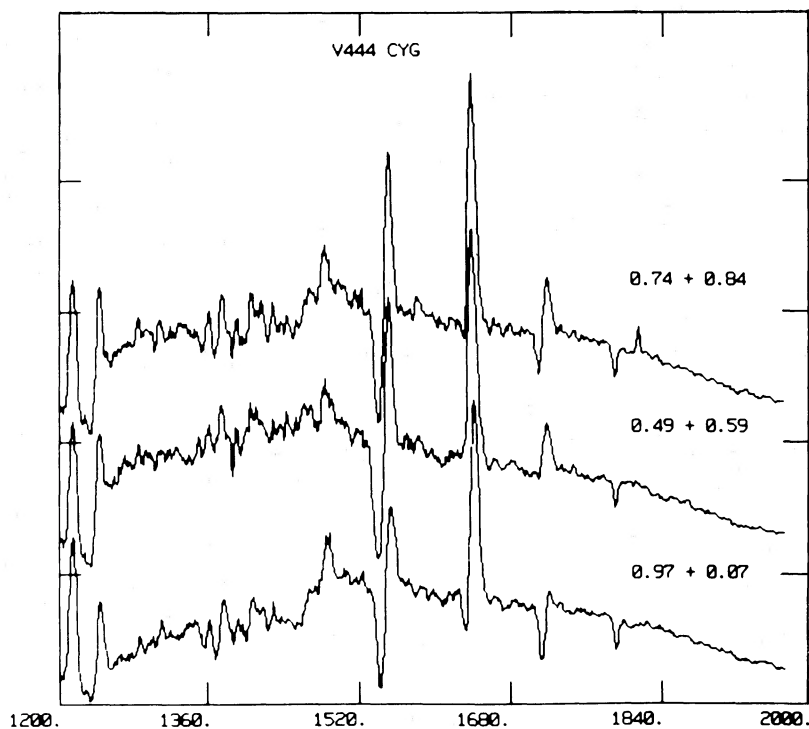
^a Velocities in units 10^2 km s^{-1} .^b Fluxes in units of $10^{-13} \text{ ergs cm}^{-2} \text{ s}^{-1} \text{ \AA}^{-1}$.^c Equivalent widths in units of angstroms.^d Phases in parentheses have large uncertainties.

FIG. 1a.—IUE spectra of V444 Cyg. Spectra at similar phases have been averaged, and their phases indicated.

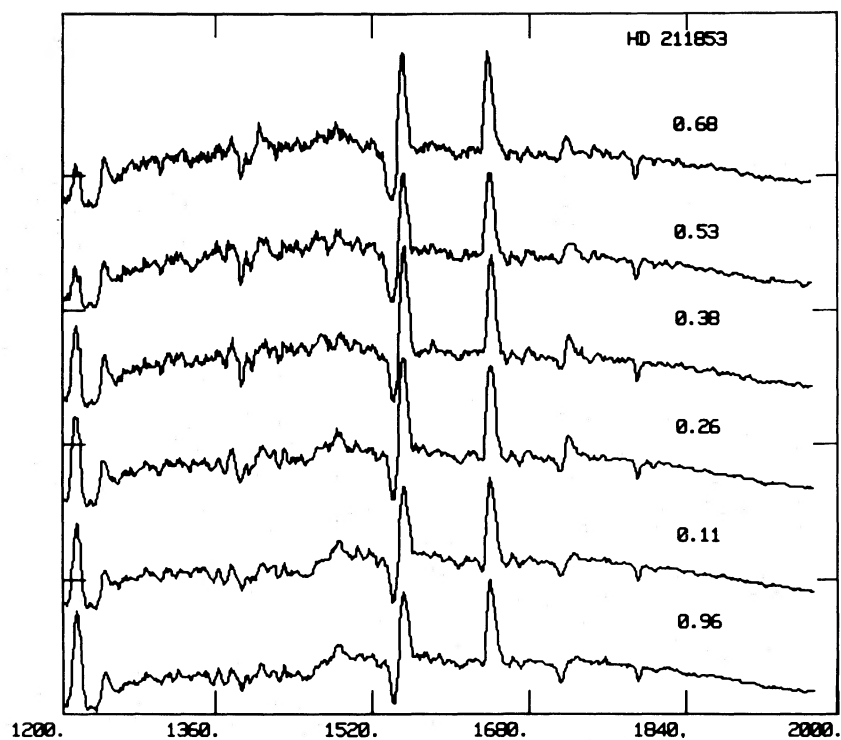


FIG. 1b.—IUE spectra of HD 211853

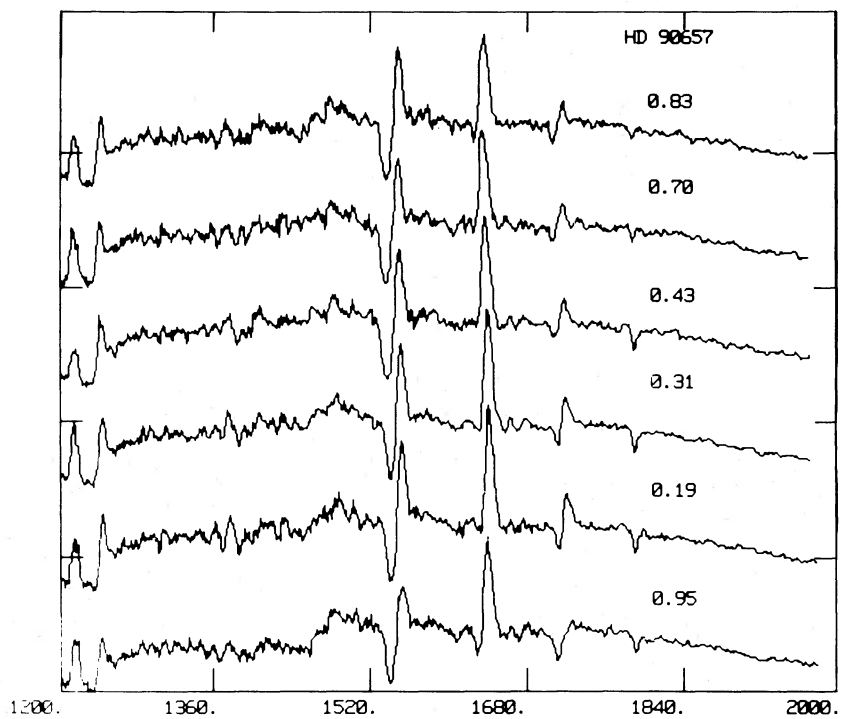


FIG. 1c.—IUE spectra of HD 90657

TABLE 3
MEANS AND STANDARD DEVIATIONS OF QUANTITIES IN TABLE 2

| Target | $\langle V_A \rangle^a$ | $\langle V_E \rangle$ | $\langle F_A \rangle$ | Percent | $\langle F_E \rangle$ | Percent | $\langle F_{1825} \rangle$ | Percent | $\langle W_A \rangle$ | Percent | $\langle W_E \rangle$ | Percent |
|-----------------------|-------------------------|-----------------------|-----------------------|---------|-----------------------|---------|----------------------------|---------|-----------------------|---------|-----------------------|---------|
| V444 Cyg ^b | -11 ± 3 | +5 ± 4 | 10 ± 3 | 30 ± 21 | ± 4 | 18 | 11.9 ± 1.1 | 8 | 1.8 ± 1.5 | 80 | 3.2 ± 1.5 | 50 |
| HD 90657 | -11 ± 2 | +7 ± 4 | 6 ± 1 | 17 12 | ± 1.3 | 11 | 7.4 ± 0.1 | 1 | 2.4 ± 1.2 | 50 | 2.7 ± 1.2 | 50 |
| HD 94546 | -13 ± 3 | +4 ± 2 | 4.5 ± 0.4 | 10 9 | ± 0.8 | 6 | 4.4 ± 0.1 | 3 | 0.8 ± 0.6 | 80 | 6.1 ± 0.6 | 10 |
| HD 186943 | -16 ± 3 | +4 ± 3 | 6.8 ± 0.8 | 12 13.3 | ± 0.8 | 6 | 7.3 ± 0.1 | 2 | 1.1 ± 0.8 | 70 | 5.1 ± 0.4 | 10 |
| HD 211853 | -11 ± 2 | +12 ± 5 | 11 ± 3 | 27 19 | ± 2 | 11 | 12.5 ± 0.6 | 5 | 1.6 ± 0.9 | 58 | 3.2 ± 1.3 | 40 |
| HD 193077 | -11 ± 0.7 | 4 ± 0.8 | 28 ± 1 | 4 64 | ± 2 | 3 | 31.2 ± 0.3 | 1 | 1.3 ± 0.1 | 10 | 5.7 ± 0.3 | 5 |

^a Units as in Table 2.

^b Data only for the six SWP images obtained in our observing run.

tions greater than 8% occur in the 1825 Å continuum region in the same images.

4. The emission component of C iv $\lambda 1550$ shows a decrease in intensity at $\phi \approx 0$, but at the same time the absorption component is narrower instead of broader and deeper, as occurs with the N iv $\lambda 1718$ line.

As already mentioned, the strongest line variations are seen to occur in V444 Cyg, HD 90657, and HD 211853, although a more complete phase coverage of the other two sources may disclose similar degrees of variability. There is no evidence for continuum variations at $\lambda \gtrsim 1500$ Å in any of the sources except V444 Cyg, where the additional images obtained at $\phi = 0$ display variations consistent with the 30% eclipses observed in the optical region (4200–7500 Å; Cherepashchuk and Khaliullin 1973). The V444 Cyg continuum eclipse is significant only at $\phi = 0.0 \pm 0.03$; however, the variations at emission-line frequencies occur over a wider phase interval.

The changes in line structure occur smoothly as a function of orbital phase as shown in Figures 2a and 2b, where the phase dependence of the 1718 Å emission and absorption equivalent widths, respectively, is shown. The systems V444 Cyg, HD 90647, HD 211853, and HD 186943 are represented with different symbols. The similarity of the variation in the absorption components is particularly striking and suggests that the WN winds are very similar.

The ratio W_A/W_E as a function of orbital phase is shown in Figure 2c. The filled-in square represents the value of this ratio derived from the HD 193077 spectrum. The spectrum of this star is essentially that of any unperturbed W-R, so its W_A/W_E value can be used for comparison with other sources. In the four variable sources, the N iv $\lambda 1718$ line is indeed altered by enhanced absorption during orbital phases $0.8 \lesssim \phi \lesssim 1.2$, and perhaps reduced absorption at the opposite phases (i.e., $\phi \approx 0.5$). The ratios are equal to the HD 193077 value at elongations, as expected since the column density of W-R wind material projected onto the O star is small at these phases.

IV. OPTICAL DEPTH DISTRIBUTION

Because the dominant mechanism responsible for the observed variations at emission-line frequencies is the absorption of the O star's radiation by atoms in the W-R wind, one can directly obtain the optical depth along the line of sight to the O star as a function of impact parameter as

$$\tau = -\ln \left[\frac{F_A(\phi)}{F_C(\phi)} \right] - 0.2,$$

where $F_A(\phi)$ is the measured flux at orbital phases $0.75 \lesssim \phi \lesssim 1.25$ and $F_C(\phi)$ is the corresponding continuum flux. There is an intrinsic contribution to the P Cygni absorption arising in the W-R wind from absorption of the W-R core continuum radiation. Thus, a factor 0.2 is subtracted to account for this contribution to the absorption at V_A . This value is taken from measurements of F_A/F_C in HD 193077 and HD 94546, as well as at orbital phase ~ 0.7 in HD 18643. The impact parameter, p , can be related to the orbital phase and the inclination of the orbital plane i by

$$p = a[\sin^2(2\pi\phi) + \cos^2(2\pi\phi) \cos^2 i]^{1/2},$$

where a is the orbital separation.

The resulting values of τ listed in Table 4 for V444 Cyg, HD 90657, and HD 186943 are plotted in Figure 3 as a function of impact parameter. The error bars correspond to the propagated uncertainties in flux measurements.

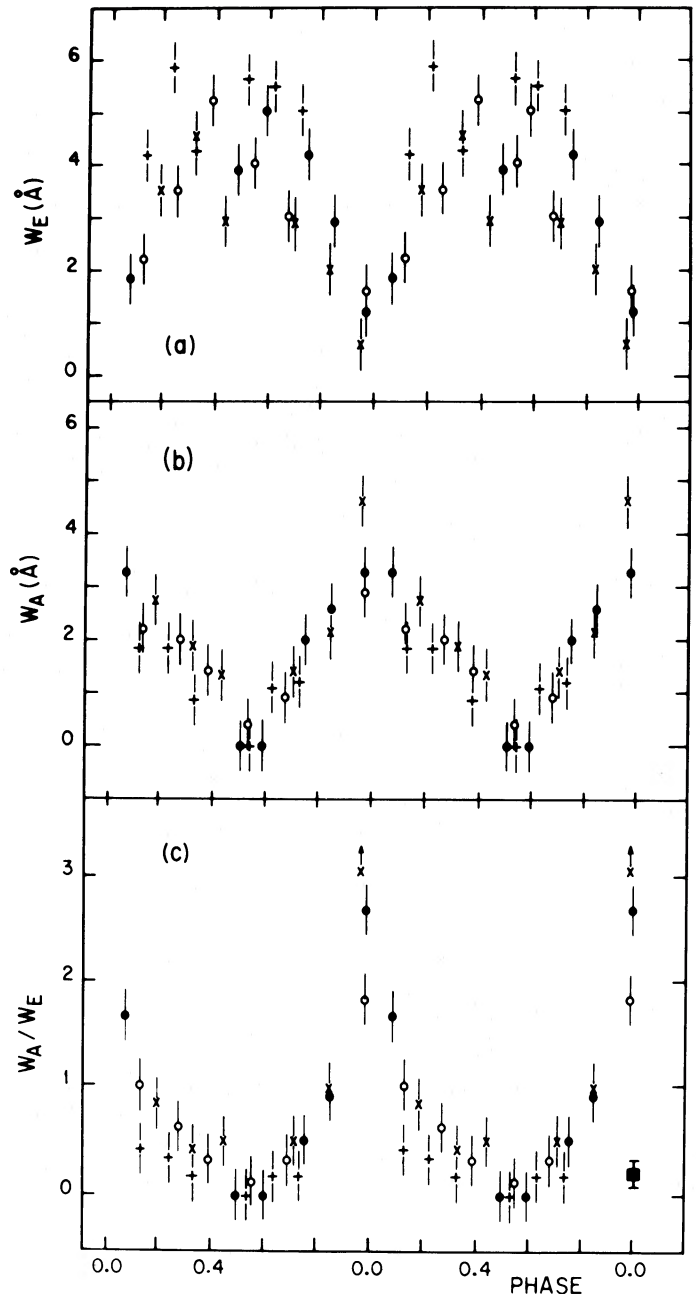


FIG. 2.—Equivalent widths of (a) emission and (b) absorption, components of N iv $\lambda 1718$ as function of orbital phase. (c) Ratio of absorption to emission. Observations for all systems are plotted. The symbols used are filled circles (●) for V444 Cyg, open circles (○) for HD 211853, crosses (×) for HD 90657, pluses (+) for HD 18643, and a filled square (■) for the nonvarying HD 193077.

The curve in Figure 3 represents a least mean squares fit to the data at $p > 14 R_\odot$. Thus, as a first approximation, the line optical depth distribution in WN winds appears to be of the form $\tau \propto p^{-1}$ for $p < 14 R_\odot$.

It is interesting to note that $\tau > 0$ for impact parameters as large as $\sim 60 R_\odot$, which means that the N iv ionization stage exists at least out to this distance from the W-R core. Castor and van Blerkom (1970) found that the He II emitting region in the WN6 star HD 192163 extends out to $70 R_\odot$. Assuming that this result is applicable to our WN 4–6 stars, we are led to

TABLE 4
PHASE DEPENDENCE OF OPTICAL DEPTH

| SWP | Phase | $P(R_{\odot})$ | $\tau(p)$ |
|------------|-------|----------------|-----------|
| V444 Cyg | | | |
| 13832..... | 0.917 | 19.0 | 0.51 |
| 15380..... | 0.852 | 29.0 | 0.17 |
| 15387..... | 0.992 | 7.6 | 0.77 |
| 15388..... | 0.998 | 7.4 | 0.72 |
| 15389..... | 0.003 | 7.5 | 0.77 |
| 15390..... | 0.008 | 7.6 | 0.77 |
| 15391..... | 0.015 | 8.1 | 0.62 |
| 15392..... | 0.020 | 8.6 | 0.72 |
| 15394..... | 0.030 | 9.9 | 0.62 |
| 15396..... | 0.051 | 13.5 | 0.77 |
| 15397..... | 0.056 | 14.2 | 0.64 |
| 15399..... | 0.066 | 15.9 | 0.64 |
| 15400..... | 0.071 | 16.8 | 0.60 |
| 15401..... | 0.076 | 17.7 | 0.62 |
| 15402..... | 0.081 | 18.6 | 0.53 |
| 15403..... | 0.085 | 19.3 | 0.64 |
| 15406..... | 0.103 | 22.4 | 0.56 |
| 15407..... | 0.108 | 23.2 | 0.53 |
| 15408..... | 0.114 | 24.1 | 0.47 |
| 15588..... | 0.835 | 31.0 | 0.29 |
| 15602..... | 0.073 | 17.2 | 0.53 |
| 15644..... | 0.974 | 9.4 | 0.49 |
| HD 90657 | | | |
| 15584..... | 0.83 | 49 | 0.19 |
| 15598..... | 0.95 | 25 | 0.40 |
| 15618..... | 0.19 | 51 | 0.11 |
| HD 186943 | | | |
| 15578..... | 0.11 | 47 | 0.2 |
| 15586..... | 0.22 | 67 | 0.2 |

conclude that ions with different ionization potentials do indeed coexist in WN winds, as concluded by Willis (1982).

Figure 3 provides only a crude approximation to the actual optical depth distribution in the WN winds for several reasons. First, we are disregarding the finite size of the O star's continuum emitting core, which in the case of V444 Cyg has a radius

of $\sim 10 R_{\odot}$. Thus, assuming a uniform distribution across the O star's disk, each value of τ represents the average optical depth for the interval $p \pm 10 R_{\odot}$. Second, the quantity being derived is the optical depth at V_A , the position of maximum absorption in the P Cyg profile. The material responsible for the absorption at this wavelength is not at a distance p from the W-R core since it has a net outward (toward the observer) velocity, but without a knowledge of the velocity distribution in the wind, the exact position of this absorbing material cannot be determined. A more accurate optical depth distribution can be obtained by using the rest wavelength of the emission line (Koenigsberger 1983) and spectra with higher resolution.

V. WIND-WIND COLLISIONS

In Figures 4a and 4b we have plotted the ratios of the images corresponding to "W-R in front" divided by "O star in front" for the five variable systems. Where possible, spectra corresponding to similar phases have been coadded to increase the signal-to-noise factor. For HD 94546 it has been necessary to construct the ratio with the spectrum corresponding to $\phi \approx 0.5$ in the numerator; i.e., inverted with respect to the other cases. We note, however, that an error of $0^{\text{d}}006$ in the orbital period, which is consistent with uncertainties in the period determination, could generate a phase shift of 0.5 when extrapolating zero phase from the initial epoch listed in Table 1 to the observations reported here.

The changes in the spectra between phases near 0.0 and 0.5 are evident in Figure 4. For example, the enhanced absorptions at $\phi \approx 0$ show up here as depressions with respect to the level of unity. That is, if there were no variations, the ratios would be equal to unity at all wavelengths. Particularly striking is the spike at $\sim 1540 \text{ \AA}$ in Fig. 4a, which results from the narrower C iv $\lambda 1550$ absorption components at $\phi \approx 0$, as compared to $\phi \approx 0.5$. Since this line corresponds to a resonance transition, it can produce significant absorption even at extremely low densities and thus, a strong contribution from the O star's wind to the overall profile is expected. The fact that the absorption is broader when the O star is in front of the W-R implies that the O star's contribution occurs at higher expansion velo-

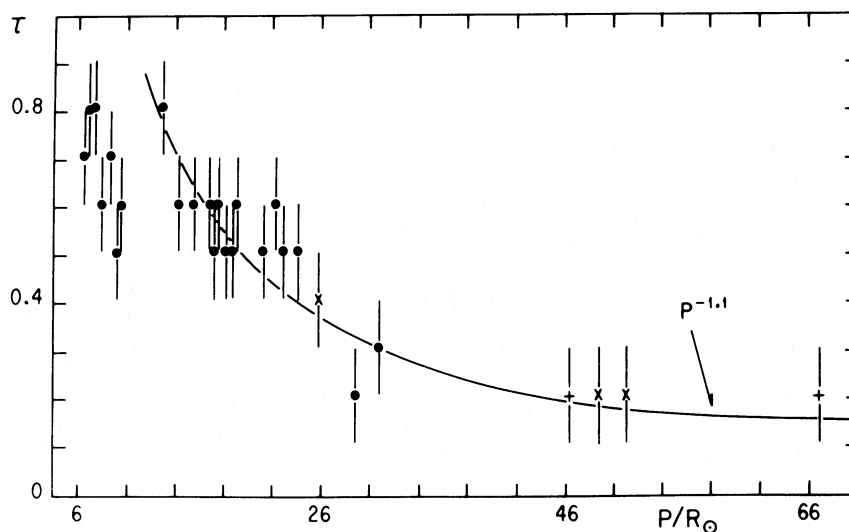


FIG. 3.—Optical depth distribution of N IV $\lambda 1718$ as a function of impact parameter. Also shown is a least-squares fit to the data at $P > 14 R_{\odot}$. Symbols as in Fig. 2.

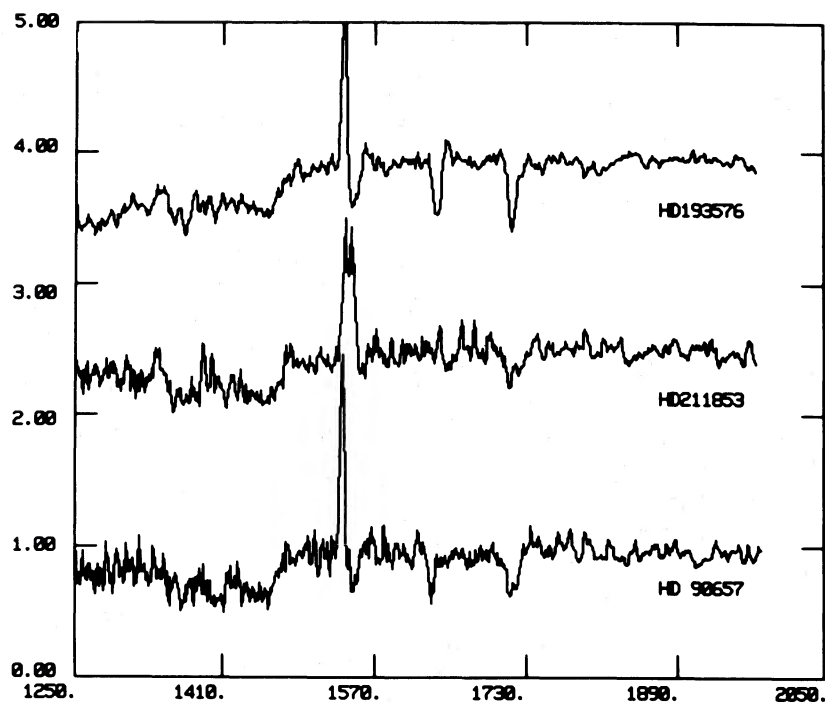


FIG. 4a

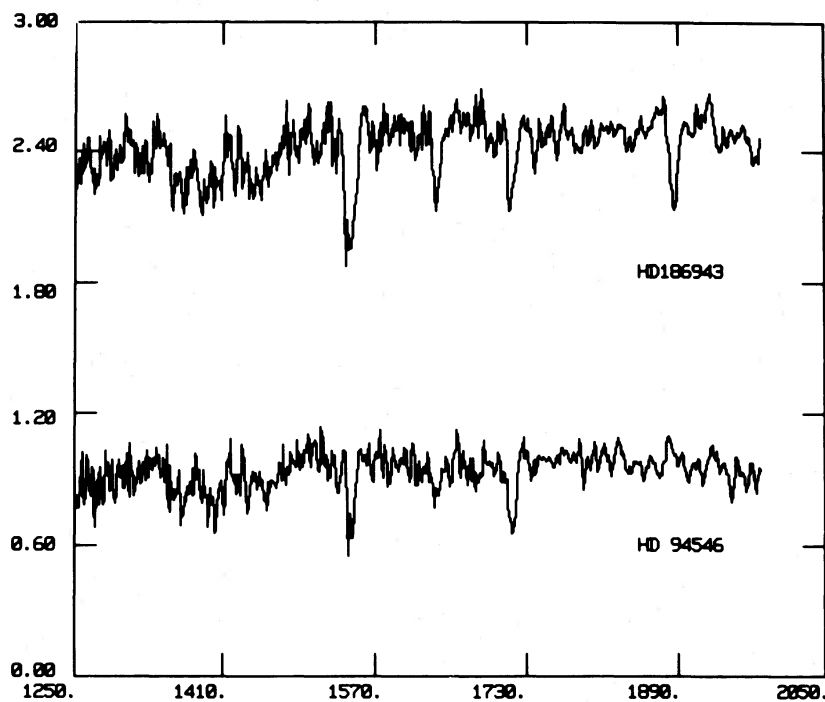


FIG. 4b

FIG. 4.—Ratios of images at phase (a) 0 and (b) 0.5, i.e., “W-R in front” and “O star in front.” Curves have been displaced vertically with respect to each other by 1.5 units.

cities than the contribution arising in the W-R wind. This means that the O star companions in the systems of Figure 4a have C IV out to higher wind velocities than do the W-Rs. Published results for terminal velocities in O stars (Garmany *et al.* 1981) also suggest that the early O stars have higher terminal velocities. Although adequate phase coverage is lacking, it may be significant that the spike is absent in the HD 18693 ratio, since this system contains the latest O-type companion of our sample.

Strong wind-wind interaction effects are indicated by the behavior of the shortward absorption edge of C IV $\lambda 1550$. The fact that the highest velocity is seen in the line when the O star is in front of the W-R, and diminishes when it is in back implies that the O star's wind structure is being affected. The physical picture is as follows:

The outflow from the W-R is more massive than that of the O star, and dominates the O star wind. When they collide, the O star wind cannot achieve its maximum velocity. Thus, the spikes in Figure 4a provide observational evidence for wind-wind collisions in WR + O binaries.

VI. POSSIBLE Fe V AND Fe VI CONTRIBUTIONS

With the exception of V444 Cyg at orbital phases $\phi = 0.00 \pm 0.03$, no appreciable changes in the continua at $\lambda > 1550 \text{ \AA}$ occur in our SWP images nor in LWR (long wavelength redundant, 1900–3300 \AA) spectra of HD 211853 and HD 186943 (Hutchings and Massey 1983). However, changes shortward of 1500 \AA are significant, especially in systems of Figure 4a. These changes are approximately of the same magnitude as those in N IV $\lambda 1718$, and have the same phase dependence. Thus, it is very probable that they result from line variability. That is, closely spaced, numerous lines all behaving in the same manner would, given their Doppler broadening, produce the observed effects. In fact, there is a large concentration of lines at $\lambda < 1550 \text{ \AA}$, most of them due to transitions of Fe v and Fe vi ions, as a search through published line lists (Reader *et al.* 1980; Ekberg 1975a, b; Ekberg and Edlen 1978) shows. Specifically, Fe v has 236 lines within the wavelength interval 1300–1500 \AA , but only 78 weak lines between 1500–1700 \AA . The strongest lines all lie between 1350 and 1486 \AA . Fe vi has no transitions at wavelengths greater than 1500 \AA , and all its strong ones lie shortward of 1380 \AA . It is also worth noting that Fe v has the same ionization potential as N IV, thus making its existence in the WN 4–6 winds very reasonable.

Lines of Fe v have been identified in the spectra of the binary UW CMa (Drechsel *et al.* 1981), two W-Rs (Fitzpatrick 1982),

and an O-type subdwarf (Bruhweiler, Kondo, and McCluskey 1981), although in the latter three objects they are presumably photospheric absorptions.

We thus conjecture that the apparent continuum variations shortward of 1550 \AA in our IUE images are due to variations of weak lines, with the major contributors being Fe v and Fe vi. Any line with an adequately populated lower level would cause absorption of the O star's continuum, but only Fe v and Fe vi have the sufficient number of lines to generate a pseudo-continuum.

VII. CONCLUSIONS

The objectives of this investigation have been to analyze the variability of W-R binaries (WN + O) in the ultraviolet spectral region 1200–1900 \AA and determine whether the periodic, phase-dependent variations can be used to empirically derive the physical properties of the WN winds. We have found the variations in the UV to be similar in nature to those observed in the optical spectra. That is, there is a strengthening of absorption components in P Cygni-type features at orbital phases in which the O star is behind the W-R wind, and we find the dominant mechanism producing the variations to be selective atmospheric eclipses of the O component by the W-R wind. Based on this explanation, and empirical optical depth distribution in the WN winds of the form $\tau \propto p^{-1}$ is derived for $p \gtrsim 14 R_{\odot}$. In addition, we find that the N IV ionization stage exists at least out to $\sim 60 R_{\odot}$, consistent with the proposed constant ionization structure (Willis 1982).

Among the next steps that must be taken is the modeling of P Cygni profiles using empirically determined parameters, such as the optical depth distribution. As Castor (1970b) pointed out, W-R profiles can be modeled and reproduced with a variety of dissimilar combinations of optical depth and source functions. We propose that the additional information required to restrict the free parameters in model profiles may be obtained from optical depth analyses similar to the one we have performed.

We wish to express our gratitude to R. Panek, R. Schiffer, R. Bradley, and the IUE staff for their assistance in the observations and data reduction, and the National Space Science Data Center for providing archival data. We thank V. Niemela for communicating results prior to publication, and J. Franco, P. Massey, and D. van Blerkom for useful discussions. Comments from an anonymous referee are appreciated. This work was supported in part by grant NA5-201. G. K. holds grant No. 24033 from the Mexican National Science and Technology Council (CONACYT).

REFERENCES

- Ayres, T. R. 1982, *Ap. J.*, **257**, 243.
 Bahng, J. D. R. 1975, *Ap. J.*, **200**, 128.
 Bappu, M. K. V., and Sinhal, S. D. 1955, *Ap. J.*, **60**, 152.
 Barlow, M. J., Smith, L. J., and Willis, A. J. 1981, *M.N.R.A.S.*, **196**, 101.
 Bruhweiler, F., Kondo, Y., and McCluskey, G. E. 1981, *Ap. J. Suppl.*, **46**, 255.
 Castor, J. I. 1970a, *Ap. J.*, **160**, 1187.
 ———. 1970b, *M.N.R.A.S.*, **149**, 111.
 Castor, J. I., and van Blerkom, D. 1970, *Ap. J.*, **161**, 485.
 Cherepashchuk, A. M. 1975, *Soviet Astr.*, **19**, 47.
 ———. 1982, *Ap. Space Sci.*, **86**, 299.
 Cherepashchuk, A. M., Eaton, Y. A., and Khaliullin, F. F. 1980, in *IAU Symposium 88, Close Binary Stars: Observations and Interpretations*, ed. M. U. Plavec, D. M. Popper, and R. K. Ulrich (Dordrecht: Reidel), p. 193.
 Cherepashchuk, A. M., and Khaliullin, F. F. 1973, *Soviet Astr.*, **17**, 330.
 Cowley, A., Hiltner, W. A., and Berry, C. 1971, *Astr. Ap.*, **11**, 407.
 Creech, B. A., Fabian, A. C., and Pringle, J. E. 1978, *Nature*, **273**, 645.
 Drechsel, J., Rahe, J., Kondo, Y., and McCluskey, G. E. 1981, *Astr. Ap. Suppl.*, **45**, 473.
 Eaton, Y. A., Cherepashchuk, A. M., and Khaliullin, F. F. 1982, in *Advances in Ultraviolet Astronomy: Four Years of IUE Research* (NASA Conf. Pub. 2238, p. 542).
 Ekberg, J. O. 1975a, *Phys. Scripta*, **12**, 42.
 ———. 1975b, *Phys. Scripta*, **11**, 23.
 Erberg, J. O., and Edlen, B. 1978, *Phys. Scripta*, **18**, 107.
 Firmani, C., Koenigsberger, G., Bisiacchi, G. F., Moffat, A. F. J., and Isserstedt, J. 1980, *Ap. J.*, **239**, 607.
 Fitzpatrick, E. L. 1981, *Ap. J. (Letters)*, **261**, L91.
 Ganesh, K. S., and Bappu, M. K. V. 1968, *Kodiakanal Obs. Bull.*, No. 185.
 Garmany, C. D., Olson, G. L., Conti, P. S., and van Steenberg, M. 1981, *Ap. J.*, **250**, 660.
 Hiltner, W. A. 1945, *Ap. J.*, **99**, 273.
 Hutchings, J. B., and Massey, P. 1983, *Pub. A.S.P.*, **95**, 151.
 Jeffers, S., Weller, W., and Sanyal, A. 1973, *Nature Phys. Sci.*, **243**, 109.
 Khaliullin, F. F. 1973, *Soviet Astr.*, **16**, 636.
 Khaliullin, F. F., and Cherepashchuk, A. M. 1976, *Soviet Astr.*, **20**, 186.
 Koenigsberger, G. 1983, Ph.D. thesis, Pennsylvania State University.

- Kuhi, L. V. 1968, *Ap. J.*, **152**, 89.
 ———. 1973, in *IAU Symposium 49, Wolf-Rayet and High-Temperature Stars*,
 ed. M. K. V. Bappu and J. Sahade (Dordrecht: Reidel), p. 205.
 Lamontagne, R., et al. 1982, *Ap. J.*, **253**, 230.
 Massey, P. 1981, *Ap. J.*, **253**, 230.
 Massey, P., and Niemela, V. 1981, *Ap. J.*, **245**, 195.
 Münch, G. 1950, *Ap. J.*, **112**, 266.
 Niemela, V. 1976, *Ap. Space Sci.*, **45**, 191.
 Niemela, V., and Moffat, A. F. J. 1982, *Ap. J.*, **259**, 213.
 Panek, R. 1981, *IAU Newsl.*, No. **18**, 68.
 Prilutskii, O. F., and Usov, V. V. 1976, *Soviet Astr.*, **20**, 2.
 Reader, J., Corliss, C. H., Wiese, W. L., and Martin, G. A., 1980, *Wavelengths
 and Transition Probabilities for Atoms and Atomic Ions* U.S. Department of
 Commerce, NBS 68.
 Rublev, S. V. 1961, *Soviet Astr.*, **4**, 780.
 ———. 19663, *Soviet Astr.*, **6**, 686.
 Sahade, J. 1958, *Mém. Soc. Roy. Liège*, 4c Sér., **20**, 46.
 Willis, A. J. 1982, *M.N.R.A.S.*, **198**, 897.
 Willis, A. J., Wilson, R., Macchetto, F., Beeckmans, F., Van der Hucht, K. A.,
 and Strickland, D. J. 1979, in *The First Year of IUE*, ed. A. J. Willis
 (London: University College), p. 259.
 Wilson, O. C. 1945, *Ap. J.*, **91**, 379.

L. H. AUER: Los Alamos National Laboratory, P.O. Box 1663, Mail Stop F665, Los Alamos, NM 87545

G. KOENIGSBERGER: University of Mexico, Instituto Astronomia, APDO. Postal 70-264, Mexico City, Mexico D.F.